Kinetic and Magnetic Resonance Studies of Active-Site Mutants of Staphylococcal Nuclease: Factors Contributing to Catalysis†

Engin H. Serpersu, David Shortle, and Albert S. Mildvan*

Department of Biological Chemistry, The Johns Hopkins University School of Medicine, Baltimore, Maryland 21205

Received August 5, 1986; Revised Manuscript Received November 4, 1986

ABSTRACT: To determine the origin of the overall $\sim 10^{16}$-fold rate enhancement of DNA hydrolysis catalyzed by staphylococcal nuclease, the effects of single mutations that alter the amino acid residue at each of the essential positions Asp-21, Asp-40, Thr-41, Arg-35, and Arg-87 have been examined. Metal ion and substrate analogue binding were quantitated by EPR, by the paramagnetic effects of Mn^{2+} on $1/T_1$ of water protons, and by fluorescence titrations, yielding the six dissociation constants of the ternary enzyme–Mn^{2+}–3′,5′-pdTp and enzyme–Ca^{2+}–3′,5′-pdTp complexes. The kinetic parameters k_{cat}, K_A^{Ca}, K_M^{Ca}, K_S^{DNA}, K_M^{DNA}, and K_I^{Mn} were determined by monitoring the rate of DNA hydrolysis. By thermodynamic and kinetic criteria, Mn^{2+} binds tightly to the Ca^{2+} binding site of the enzyme but is at least 36 000-fold less effective than Ca^{2+} in activating the enzyme. Alterations of the liganding residues in the D40G, D40E, T41P, D21E, and D21Y mutants generally weaken the binding of Ca^{2+} $\leq$12.7-fold and of Mn^{2+} $\leq$5.4-fold, exert little effect on the K_S^{DNA} or K_M^{DNA} ($\leq$3.2-fold), and raise the affinity of the enzyme and its metal complexes for 3′,5′-pdTp by factors $\leq$13.5-fold. Small changes in the ligand geometry are also reflected in the Mn^{2+} complexes of the liganding mutants (i.e., those in which the metal-liganding amino acids have been altered) by decreases in the electron-spin relaxation time of Mn^{2+}. Inhibitory effects on k_{cat} are noted in all of the liganding mutants with D40E, D40G, T41P, D21E, and D21Y showing 12-, 30-, 37-, 1500-, and $\geq$29 000-fold reductions, respectively. The $\geq 10^3$-fold larger inhibitory effects on k_{cat} of enlarging Asp-21 as compared to enlarging Asp-40 are ascribed to the displacement of the adjacent water molecule which attacks the phosphodiester. Mutations of each of the essential Arg residues to Gly (R35G and R87G) reduce k_{cat} by factors $\geq$35 000 but weaken metal binding $\leq$9-fold. While R35G and its metal complexes bind 3′,5′-pdTp only very weakly, consistent with Arg-35 functioning as a hydrogen-bond donor to the phosphodiester substrate, the identical alteration of Arg-87 does not significantly change the affinity of the enzyme or its metal complexes for the substrate analogue 3′,5′-pdTp, in contrast to its described role in binding either 3′,5′-pdTp or the phosphodiester substrate. A revised mechanism for staphylococcal nuclease is proposed in which Arg-87 interacts only with the trigonal bipyramidal transition state rather than with the ground state of the bound substrate. Since the active-site mutations studied reduce k_{cat} by factors approaching 10^5, and yet alter metal ion and substrate analogue binding by at most 1 order of magnitude (except for R35G), we argue that these mutations do not greatly perturb the native conformation of the enzyme and that their effects on k_{cat} can therefore be interpreted quantitatively in terms of specific changes in the chemistry of the catalytic events. Hence, the 10^{16}-fold rate acceleration produced by staphylococcal nuclease may result from the product of the following factors: metal catalysis by Ca^{2+} ($\geq 10^{4.6}$); transition-state stabilization by Arg-87 ($\geq 10^{4.6}$); catalysis by approximation of the attacking water ($\geq 10^3$); and general base catalysis ($\sim 10^4$).

Staphylococcal nuclease efficiently catalyzes the hydrolysis of phosphodiester linkages in DNA and RNA to yield 3′-mono- and dinucleotides (Figure 1; Tucker et al., 1979). A comparison of k_{cat}, the maximal turnover number of this enzyme (95 s^{-1}; Serpersu et al., 1986b), with the pseudo-first-order rate constant for the nonenzymatic hydrolysis of phosphodiesters, extrapolated to 24 °C and pH 7.4 (5.7×10^{-14} s^{-1}; Kumamoto et al., 1955; Bunton et al., 1960), indicates a rate acceleration by staphylococcal nuclease of (1.7×10^{15})-fold. A somewhat larger rate enhancement by this enzyme, $\geq 10^{16}$-fold, may be more appropriate, since k_{cat} may be limited in part by steps other than bond breaking (Sulkowski & Laskowski, 1968; Dunn et al., 1973; Tucker et al., 1978). A chemical mechanism for staphylococcal nuclease, proposed on the basis of the 1.5-Å X-ray structure of the ternary enzyme–Ca^{2+}–pdTp complex (Cotton et al., 1979) and the extensive kinetic studies with the intact and semisynthetic enzymes (Anfinsen et al., 1971; Chaiken & Sanchez, 1972), is shown in Figure 2. In this mechanism, the essential Ca^{2+} activator is bound in an octahedral complex, receiving three cis ligands from the protein, Asp-21, Asp-40, and the amide carbonyl group of Thr-41, as well as a phosphodiester oxygen of the substrate. The phosphodiester group is also believed to be held by Arg-35 and Arg-87, each operating as a bifunctional hydrogen-bond donor, as found in X-ray studies of model guanidinium phosphate complexes (Cotton et al., 1974). The attacking water molecule is either the inner-sphere ligand or, as proposed by Cotton et al. (1979), the second-sphere ligand of Ca^{2+}, adjacent to-Asp 21. While both of these water molecules are close enough to the reaction-center phosphorus to attack it in an associative mechanism (4.0 and 3.5 Å, respectively), as found by computer graphics, only the second-sphere water molecule is close enough to Glu-43 to donate a hydrogen bond to this residue, which would permit Glu-43 to function as a general base (Cotton et al., 1979). Evidence for such a role for Glu 43 is the $>10^2$-fold lower activity of the Glu-43 to Asp (E43D) variant of the semisynthetic enzyme

† This work was supported by National Institutes of Health Grants AM28616 and GM34171.

0006-2960/87/0426-1289$01.50/0

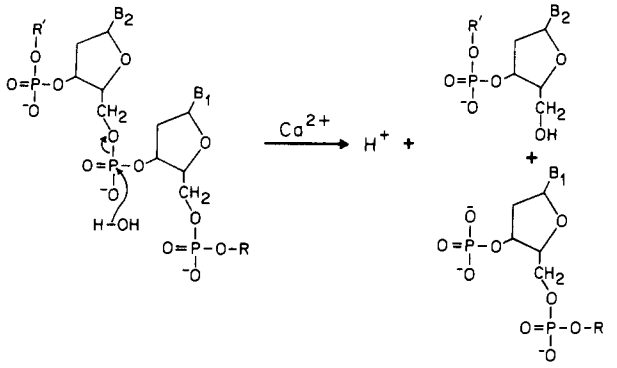

FIGURE 1: Reaction catalyzed by staphylococcal nuclease. Nucleophilic substitution by water on the phosphodiester phosphorus of DNA or RNA yields the 3′-mono- or 3′-dinucleotide.

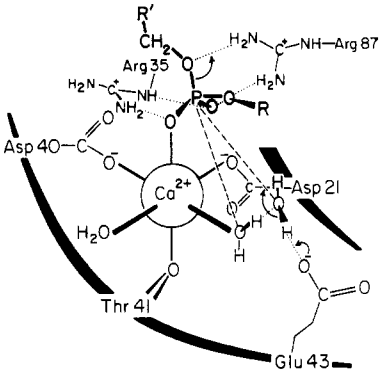

FIGURE 2: Mechanism of staphylococcal nuclease based on the 1.5-Å X-ray structure (Cotton et al., 1979) and kinetic studies (Anfinsen et al., 1971).

(Chaiken & Sanchez, 1972) and the 10^3–10^4-fold lower activities of the E43D, E43N, and E43Q mutants (Hibler & Gerlt, 1986).

This paper reports a detailed examination of the kinetic and thermodynamic effects of selected genetic alterations of the metal-liganding and substrate binding residues of staphylococcal nuclease. Our findings require a modification of the mechanism of Figure 2 and permit us to evaluate the quantitative contribution of each of the active-site components to catalysis. A preliminary report of this work has been published (Serpersu et al., 1986a).

Experimental Procedures

Materials

The nucleotide 3′,5′-pdTp was purchased from P-L Biochemicals. Before use, all buffer and nucleotide solutions were passed over Chelex 100 resin to remove trace metals. Salmon sperm DNA was obtained from Sigma, and DNA used in the enzyme assays was denatured by heating for 30 min at 100 °C, followed by rapid cooling on ice (Cuatrecasas et al., 1967a).

Methods

Enzyme Assay. The enzymatic activity was measured by observing the absorbance increase at 260 nm as DNA is hydrolyzed (Cuatrecasas et al., 1967a). One unit of enzymatic activity is defined as the amount of enzyme causing a change of 1.0 absorbance unit per minute at 260 nm in a 1-cm cell. Protein concentrations were determined by the absorbance at 280 nm ($\epsilon_{1cm}^{0.1\%} = 0.93$ at neutral pH) (Dunn et al., 1973; Tucker et al., 1978) with the exception of the D21Y mutant for which the Bradford method (Bradford, 1976) was used with the wild-type staphylococcal nuclease as standard. The assay mixture consisted of the indicated amounts of DNA and Ca^{2+} in 40 mM tris(hydroxymethyl)aminomethane hydrochloride (Tris-HCl),[1] pH 7.4, in a volume of 1.0 mL at 24 ± 1 °C. To this mixture 0.45–0.54 μg of D40E, 2.9–3.2 μg of T41P, or 10.4–12.8 μg of D21E was added to start the reaction. Velocity was determined from the linear portions of the recorder trace and expressed as the change in absorbancy per minute per microgram of protein. Enzymatic activities were linear with the amount of protein used in the assays. In the kinetic experiments with Mn^{2+} as inhibitor, the concentration of free Mn^{2+} was estimated by assuming 0.38 ± 0.04 Mn^{2+} binding site per DNA phosphorus with a dissociation constant of 68 μM (Slater et al., 1972).

Although staphylococcal nuclease has a pH optimum in the range of 8.6–10.3, depending on the concentration of Ca^{2+} (Tucker et al., 1978), we have determined the kinetic parameters of all the mutant enzymes at pH 7.4 to permit kinetic and binding studies with Mn^{2+} since $Mn(OH)_2$ precipitates at higher pH values. These conditions were also necessary to compare the results of the present work with our previous kinetic and magnetic resonance studies of both wild-type enzyme and the D40G mutant enzyme (Serpersu et al., 1986b).

A semiquantitative assay of staphylococcal nuclease, based on the color change of a metachromatic dye upon the hydrolysis of DNA, as the nuclease diffuses through an agar gel (Lachica et al., 1971; Shortle, 1983) was used to detect the very low enzymatic activities of the D21Y, R35G, and R87G mutants. A range of dilutions of the mutant enzymes was spotted in 2-μL volumes onto a freshly prepared petri plate containing 10 mL of agar gel consisting of 50 mM Tris-HCl, pH 9.0, 1% NaCl, 1% Difco agar, 300 μg/mL boiled salmon sperm DNA, and 0.2 mg/mL toluidine blue O. Plates were then incubated for 3 h at 30 °C, and the diameters of the pink halos formed by the diffusing active enzymes were measured with a transparent ruler. The dilutions of wild-type enzyme were adjusted to give halos with diameters equal to those produced by the mutant enzymes, in order to compare relative activities.

Analysis of Kinetic Data. The data obtained from the spectrophotometric enzyme assay were plotted in double-reciprocal form as initial velocity vs. the concentration of free Ca^{2+} and as initial velocity vs. the concentration of DNA as previously described (Serpersu et al., 1986b). The following secondary plots were made from these two primary plots to obtain K_A^{Ca}, K_M^{DNA}, K_S^{DNA}, and K_M^{Ca} for the mutant enzymes D40E, T41P, and D21E. (A) The reciprocals of the apparent K_M^{Ca} values were plotted against the DNA concentration. Extrapolation to zero DNA concentration yielded the activator constant of Ca^{2+} (K_A^{Ca}). (B) The extrapolated apparent V_{max} values at infinite free Ca^{2+} concentration and finite DNA concentrations were plotted against the DNA concentrations in double-reciprocal form. From the intercepts on the ordinate and the abscissa, V_{max} and K_M^{DNA}, respectively, were obtained. (C) Reciprocals of the apparent K_M^{DNA} values were plotted against the free Ca^{2+} concentration. Extrapolation to zero Ca^{2+} concentration yielded the dissociation constant of the binary enzyme–DNA complex (K_S^{DNA}). (D) Extrapolated apparent V_{max} values at infinite DNA and finite Ca^{2+} concentrations were plotted against the free Ca^{2+} concentration in double-reciprocal form. The intercept on the ordinate yielded a duplicate value of V_{max} which agreed with the V_{max}

[1] Abbreviations: 3′,5′-εpAp, 1,N^6-ethenoadenosine 3′,5′-bisphosphate; Tris-HCl, tris(hydroxymethyl)aminomethane hydrochloride; SDS-PAGE, sodium dodecyl sulfate–polyacrylamide gel electrophoresis.

Table I: Kinetic Parameters of the Wild-Type and Active-Site Mutants of Staphylococcal Nuclease[a]

enzyme[b]	relative V_M	K_A^{Ca} (mM)	K_M^{Ca} (mM)	K_S^{DNA} (μg/mL)[c]	K_M^{DNA} (μg/mL)[c]	K_I^{Mn} (μM)
WT	1.0[d]	0.460 ± 0.06	0.110 ± 0.02	17.9 ± 0.7	3.50 ± 0.8	6.8 ± 4.2
D40G	3.3×10^{-2}	3.44 ± 0.36	1.13 ± 0.07	27.8 ± 3.4	4.65 ± 1.25	105 ± 15
D40E	8.1×10^{-2}	3.83 ± 1.6	1.75 ± 0.14	15.9 ± 2.6	4.98 ± 0.93	1.6 ± 0.4
T41P	2.7×10^{-2}	1.49 ± 0.41	0.93 ± 0.07	20.0 ± 5.6	11.3 ± 1.85	13.0 ± 1.5
D21E	6.7×10^{-4}	1.1 ± 0.6	0.48 ± 0.06	18.0 ± 8.0	5.3 ± 1.2	33 ± 9
D21Y	$\leq 3.5 \times 10^{-5}$					
R87G	$\leq 2.8 \times 10^{-5}$					
R35G	$\leq 2.8 \times 10^{-5}$					

[a] The data for D21E are from Figure 3. For the wild-type enzyme and for D40G, the data are from Serpersu et al. (1986b). For the other active mutants, the data are not shown. K_M^{Ca} is the Michaelis constant of Ca^{2+} at saturating [DNA], K_M^{DNA} is the Michaelis constant of DNA at saturating [Ca^{2+}], K_A^{Ca} is the K_M of free Ca^{2+} extrapolated to zero [DNA], and K_S^{DNA} is the K_M of DNA extrapolated to zero [Ca^{2+}]. [b] WT stands for the wild-type enzyme, and the other symbols represent single mutations of the respective residues as follows: D40G, Asp-40 → Gly; D40E, Asp-40 → Glu; T41P, Thr-41 → Pro; D21E, Asp-21 → Glu; D21Y, Asp-21 → Tyr; R87G, Arg-87 → Gly; and R35G, Arg-35 → Gly. [c] For comparison with K_S^{pdTp} and K_3^{pdTp} (Table III), the factor 0.715 converts these values to micromolar, assuming the molecular weight of the substrate to be an average tetranucleotide of molecular weight 1400. [d] V_{max} of the wild-type enzyme is 0.714 $\Delta A/(\mu g \cdot min)$ at pH 7.4 at 24 °C which can be expressed as $k_{cat} = 95\ s^{-1}$, assuming the molecular weight of the substrate to be an average tetranucleotide of molecular weight 1400 and $\Delta A = 0.3$ for the complete hydrolysis of 50 μg/mL DNA (Cuatrecasas et al., 1967).

from the extrapolation described in (B), and the intercept on the abscissa yielded the K_M^{Ca}. In these analyses, the lines in the primary plots were computed by a weighted least-squares analysis (Cleland, 1979), and the lines in the secondary plots were computed by a linear least-squares analysis.

Isolation of the Enzymes. The preparation, isolation, genetic mapping, and sequence analysis of all of the mutations in the staphylococcal nuclease gene used in this work were carried out as previously reported (Shortle & Lin, 1985). All mutant proteins are designated by their amino acid changes relative to the wild-type enzyme, using three-symbol nomenclature in which the first letter designates the wild-type amino acid, the number designates the position of the amino acid, and the second letter designates the mutant amino acid substituted at that position (Table I). Isolations of the mutant enzymes from the engineered strain of *Escherichia coli* carrying the expression plasmid pFOG405 were performed as described previously for the purification of the wild-type enzyme and the mutant enzyme D40G (Serpersu et al., 1986b).

Magnetic Resonance Measurements. The longitudinal and transverse relaxation rates of water protons were measured with a Seimco pulsed NMR spectrometer equipped with a variable-frequency probe. Titrations were performed at 24.3 MHz as described previously (Mildvan & Engle, 1972) by using the 180–τ–90° pulse sequence method of Carr and Purcell (Carr & Purcell, 1954; Mildvan & Engle, 1972). The observed enhancement of the relaxation rate is defined as $\epsilon^* = (1/T_{1P}^*)/(1/T_{1P})$ where $1/T_{1P}$ is the paramagnetic contribution to the longitudinal relaxation rate in the presence (asterisk) and absence of the enzymes (Mildvan & Engle, 1972). To determine the correlation times for the Mn^{2+}–water dipolar interaction (Reuben & Cohn, 1970), $1/T_{1P}$ was measured at the following eight frequencies: 15, 19.7, 24.3, 30, 36, 42, 50, and 59.8 MHz, and $1/T_{2P}$ was determined at 24.3 MHz by using the Seimco pulsed NMR spectrometer.

The concentration of free Mn^{2+} in a mixture of free and bound Mn^{2+} was determined by electron paramagnetic resonance (Cohn & Townsend, 1954) with a Varian E-4 EPR spectrometer. The EPR and NMR data were analyzed as previously described (Mildvan & Cohn, 1963, 1966; Mildvan & Engle, 1972; Serpersu et al., 1986b) to determine the stoichiometry (n) of Mn^{2+} ions bound to each enzyme, the dissociation constant (K_D), and the enhancement (ϵ_b) of the binary enzyme–Mn^{2+} complex. Titrations of binary enzyme–Mn^{2+} complexes with 3′,5′-pdTp were analyzed by computer as previously described (Reed et al., 1970; Mildvan & Engle, 1972) to yield dissociation constants and enhancement factors (ϵ_T) of ternary complexes. In addition, the binding of Mn^{2+} to enzyme–3′,5′-pdTp complexes was monitored by EPR and by changes in $1/T_{1P}^*$ of water protons, providing independent measurements of the dissociation constants of Mn^{2+} from ternary enzyme–Mn^{2+}–3′,5′-pdTp complexes.

Fluorescence Measurements. The dissociation constants of binary complexes of staphylococcal nuclease with 3′,5′-pdTp were determined by competition with 3′,5′-ϵpAp, based on the quenching of the fluorescence of ϵpAp by the enzyme, as previously described (Serpersu et al., 1986b).

Results

Kinetics of Activation by Ca^{2+} of the Metal-Liganding Mutants of Staphylococcal Nuclease: D40E, T41P, D21E, and D21Y. As exemplified for the D21E mutant (Figure 3), the kinetic parameters have been determined for each of the metal-liganding mutants that showed measurable activity (Table I). For comparison, Table I also includes the kinetic parameters of the wild-type and the D40G mutants which we have previously reported (Serpersu et al., 1986b). The liganding mutants D40E, D40G, T41P, and D21E show V_{max} values which are reduced by factors of 12, 30, 37, and 1500, respectively, below that of the wild-type enzyme. In contrast to these large changes in V_{max}, the K_A^{Ca} and K_M^{Ca} increased, at most, by factors of 8 and 16, respectively, and the K_S^{DNA} and K_M^{DNA} increased by factors of ≤ 1.6 and ≤ 3.2, respectively. The largest effect on the K_M^{DNA} is noted in the T41P mutant which may be a manifestation of the trans effect, since the carbonyl group of residue 41 is trans with respect to the phosphodiester (Figure 2).

The D21Y mutant showed no measurable activity in the standard assay at enzyme levels up to 12.8 μg/mL, 160-fold greater than that used for studies of the wild-type enzyme. Variation of the concentration of Ca^{2+} from 0.2 μM to 50 mM, of DNA concentration from 29 to 97.5 μg/mL, and of the pH from 7.4 to 9.0 produced no detectable activity, indicating the V_{max} of the D21Y mutant to be at least 29 000-fold lower than that of the wild-type enzyme at pH 7.4 (Table I) and at least 36 000-fold lower at pH 9.0. Accordingly, the semiquantitative plate assay revealed a small amount of activity estimated as 67 000-fold lower than that of the wild-type enzyme at pH 9.0. Although the kinetic constants could not be determined for the D21Y mutant because of its low activity, direct binding studies of Ca^{2+} and of a substrate analogue to this mutant show changes in affinity of at most 1 order of magnitude (see below).[2]

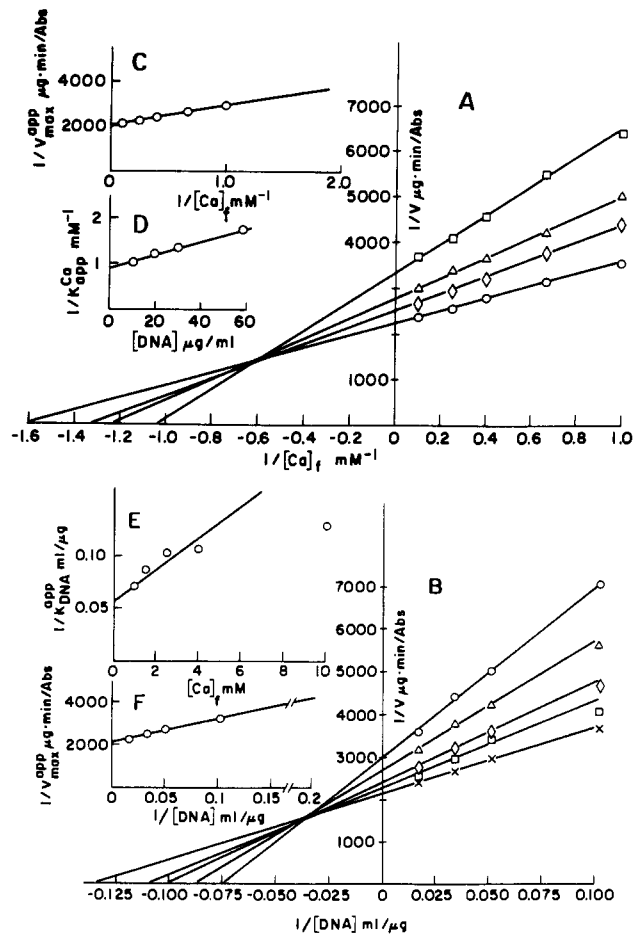

FIGURE 3: Kinetics of activation of the mutant D21E by Ca^{2+} and DNA. (A) Double-reciprocal plot of initial velocity vs. Ca^{2+} concentration. DNA concentrations in micrograms per milliliter were 9.75 (□), 19.5 (△), 29.3 (◇), and 58.5 (○). The assay medium also contained 40 mM Tris-HCl, pH 7.4. The reaction, in a total volume of 1.0 mL at 24 °C, was started by the additions of 5 μL of a solution containing 10.4 μg of D21E in the same buffer. The velocity of the reaction is defined as the absorbance change at 260 nm per microgram of enzyme per minute. (B) Double-reciprocal plot of initial velocity against DNA concentration. Free Ca^{2+} concentrations in millimolar were 1.0 (○), 1.5 (△), 2.5 (◇), 4.0 (□), and 10.0 (×). (C) Secondary plot of extrapolated apparent V_{max} values at infinite DNA concentration from (B) against free Ca^{2+} concentration in double-reciprocal form, to determine K_M^{Ca} and V_{max}. (D) Reciprocal of the extrapolated apparent K_M^{Ca} values (K_{app}^{Ca}) obtained from the intercepts on the abscissa from (A) plotted against DNA concentration, to determine the activator constant of Ca^{2+} (K_A^{Ca}) by extrapolation to zero DNA concentration. These secondary plots yielded K_M^{Ca} = 0.48 mM, V_{max} = 4.7 × 10^{-4} $\Delta A/(\mu g \cdot min)$, and K_A^{Ca} = 1.1 mM. (E) Secondary plot of the reciprocal of the extrapolated apparent K_M^{DNA} values (K_{DNA}^{app}), obtained from the intercepts on the abscissa of (B), against free Ca^{2+} concentrations which yielded, on extrapolation to zero $[Ca^{2+}]$, the dissociation constant of the enzyme–DNA complex (K_S^{DNA}) as 18.0 μg/mL. (F) Secondary plot of the extrapolated apparent V_{max} at infinite Ca^{2+} concentration (V_{max}^{app}) against DNA concentration in double-reciprocal form, which yielded K_M^{DNA} = 5.3 μg/mL and V_{max} = 4.8 × 10^{-4} $\Delta A/(\mu g \cdot min)$. In the primary plots, the data points are shown together with the lines computed by a weighted least-squares analysis (Cleland, 1979), and in the secondary plots, the lines are computed by a linear least-squares analysis.

Kinetic Effects of Mn^{2+} on the Liganding Mutants. As previously found with wild-type staphylococcal nuclease and with the D40G mutant (Serpersu et al., 1986b), no activation by Mn^{2+} was detected over the range 0.2 μM–5.0 mM $MnCl_2$ at pH 7.4 with the D40E (128 μg/mL), T41P (167 μg/mL), D21E (9.4 μg/mL), or D21Y (12.8 μg/mL) mutants. From the error levels of these measurements, activation by Mn^{2+} is less than 0.007%, 0.016%, and 3.7% of that produced by Ca^{2+} for the mutants D40E, T41P, and D21E, respectively, and all of these rates are more than 40 000 times slower than that of the Ca^{2+}-activated wild-type enzyme. However, as previously reported for the wild-type and D40G mutants (Serpersu et al., 1986b), Mn^{2+} is a linear competitive inhibitor with respect to Ca^{2+} of the D21E, T41P, and D40E mutants, with the K_I values given in Table I. The K_I values indicate that the ternary enzyme–Mn^{2+}–DNA complexes of T41P and D21E bind Mn^{2+} 2- and 5-fold weaker, respectively, than does the ternary complex of the wild-type enzyme, while the D40E mutant binds Mn^{2+} more tightly than does wild-type staphylococcal nuclease (Table I).[3]

Table II: Dissociation Constants of Binary Complexes of Mn^{2+} and Ca^{2+} and Enhancement of Mn^{2+} Complexes

enzyme or ligand	n[e]	K_D^{Mn} or K_I^{Mn} (μM)[e]	ϵ_b[f]	K_D^{Ca} or K_I^{Ca} (μM)
wild type	0.95 ± 0.03[a]	416 ± 22[a]		
	1.00 ± 0.05[b]	460 ± 63[b]	8.4 ± 0.7	510 ± 70[c]
D40G	0.98 ± 0.07[a]	1250 ± 170[a]		
	0.83 ± 0.03[b]	1012 ± 150[b]	3.8 ± 0.5	1660 ± 300[c]
D40E	0.94 ± 0.03[a]	673 ± 37[a]		
	0.97 ± 0.09[b]	700 ± 134[b]	3.3 ± 0.2	6495 ± 500[c]
T41P	0.98 ± 0.04[a]	251 ± 24[a]		
	1.23 ± 0.08[b]	396 ± 64[b]	3.6 ± 0.3	3000 ± 180[c]
D21E	0.94 ± 0.05[a]	396 ± 39[a]		
	0.95 ± 0.06[b]	398 ± 40[b]	6.2 ± 0.4	997 ± 103[c]
D21Y	0.96 ± 0.05[a]	2300 ± 160[a]		
	0.99 ± 0.10[b]	2430 ± 470[b]	2.4 ± 0.4	3480 ± 800[c]
R35G	1.00 ± 0.05[a]	862 ± 84[a]		
	0.93 ± 0.13[b]	742 ± 115[b]	7.0 ± 0.5	3940 ± 370[c]
R87G	0.95 ± 0.05[a]	850 ± 83[a]		
	1.02 ± 0.06[b]	958 ± 93[b]	6.0 ± 0.2	4590 ± 280[c]
3′,5′-pdTp	1.60 ± 0.2[a]	474 ± 50[a]	1.7 ± 0.1	1200 ± 700[d]

[a] Determined by EPR, as in Figure 4. The parameters for the wild type and D40G are from Serpersu et al. (1986b). [b] Determined by $1/T_{1P}$* of water protons, using ϵ_b. [c] Determined by competition with Mn^{2+} measuring $1/T_{1P}$* of water protons (Figure 5). [d] Determined by competition with Mn^{2+} measuring free $[Mn^{2+}]$ by EPR (Serpersu et al., 1986). [e] n is the stoichiometry of metal binding, K_D is the dissociation constant of the binary enzyme–metal complex, and K_I is the dissociation constant of the binary metal–nucleotide complex. [f] Determined by EPR and $1/T_{1P}$* of water protons.

Mn^{2+} Binding to the Liganding Mutants of Staphylococcal Nuclease. The binary enzyme–Mn^{2+} complexes of D40E, T41P, D21E, and D21Y were studied by direct titrations of these enzymes with $MnCl_2$. At each point of the titrations, the free Mn^{2+} concentration was measured by EPR spectroscopy, and the enhancement (ϵ*) of $1/T_{1P}$ of water protons due to bound Mn^{2+} was determined by pulsed NMR. The values for the fraction of free and bound Mn^{2+} determined by EPR spectroscopy were analyzed by Scatchard plots as shown in Figure 4A which also includes data from the wild-type enzyme for comparison (Serpersu et al., 1986b). In all cases, the data could be fit by assuming a stoichiometry (n) of approximately 1 binding site for Mn^{2+} with the dissociation constants (K_D) and enhancement factors (ϵ_b) given in Table II. The Scatchard analysis of data from $1/T_{1P}$ of water protons (not shown) yielded n and K_D^{Mn} values which showed

[2] The possibility that the low activity of this mutant is due to contaminating wild-type enzyme is unlikely since the mutant enzymes were synthesized in *E. coli*. However, back-mutation or an error in protein synthesis cannot be excluded. Hence, only upper-limit values of k_{cat} are given for those mutants for which the other kinetic parameters could not be measured.

[3] Like Mn^{2+}, Co^{2+} also fails to activate wild-type staphylococcal nuclease, despite the fact that it competes with Ca^{2+}, and forms a metal bridge to the 5′-phosphate of 3′,5′-pdTp (E. H. Serpersu and A. S. Mildvan, unpublished observations).

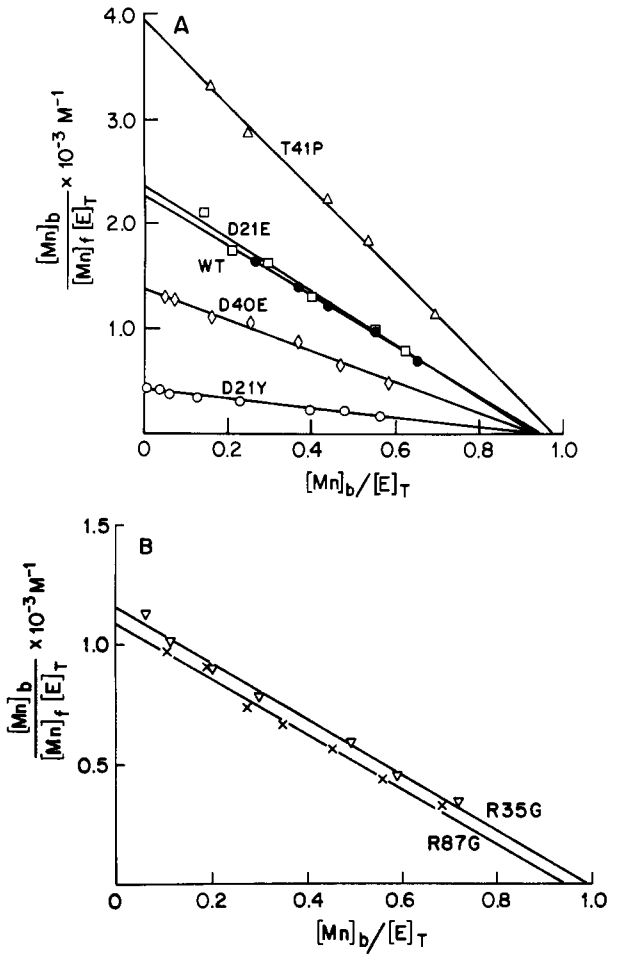

FIGURE 4: Scatchard plot of Mn^{2+} binding to wild-type staphylococcal nuclease and to the liganding and arginine mutants. (A) Titration of wild-type enzyme and the liganding mutants D21E, D21Y, D40E, and T41P with Mn^{2+}. The solutions contained 179 μM wild-type enzyme (●), 233 μM D21E (□), 432 μM D21Y (○), 328 μM D40E (◇), or 322 μM T41P (△), and 40 mM Tris-HCl, pH 7.4 at 24 °C. (B) Titration of arginine mutants R35G and R87G with Mn^{2+}. The solutions contained either 562 μM R35G (▽) or 642 μM R87G (×) and 40 mM Tris-HCl, pH 7.4 at 24 °C. The free Mn^{2+} concentrations were determined by EPR spectroscopy, and the lines show linear least-squares fits to the data points. The symbols $[Mn]_b$, $[Mn]_f$, and $[E]_T$ represent bound Mn^{2+}, free Mn^{2+}, and total enzyme concentrations, respectively.

good agreement with those measured by EPR (Table II). With the exception of the T41P and D40E mutants, weaker Mn^{2+} binding is observed with the liganding mutants than with the wild-type enzyme. With all of the liganding mutants, a lower enhancement (ϵ_b) of $1/T_{1P}$ of water protons due to enzyme-bound Mn^{2+} is seen as compared to the wild-type enzyme, most marked in the D21Y mutant. These differences reflect changes in the coordination sphere of Mn^{2+}, which will be considered in a later section.

Displacement of Mn^{2+} from the Binary Enzyme–Mn^{2+} Complexes by Ca^{2+}. The addition of Ca^{2+} to the binary enzyme–Mn^{2+} complexes of the liganding mutants decreased the observed enhancement (ϵ^*), suggesting that Ca^{2+} displaces Mn^{2+} from these complexes (Figure 5A,B). The reappearance of free Mn^{2+} was also independently observed on all samples by EPR measurements. High concentrations of Ca^{2+} displaced all of the bound Mn^{2+} in all of the liganding mutants, which is consistent with the observed competitive inhibitory behavior of Mn^{2+} in the kinetic studies (Table I). The dissociation constants of the binary enzyme–Ca^{2+} complexes (K_D^{Ca}) obtained from the concentrations of free Ca^{2+} needed to displace

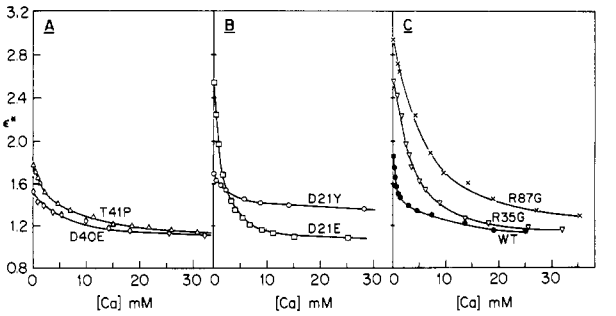

FIGURE 5: Displacement of Mn^{2+} by Ca^{2+} in binary metal complexes of wild-type, liganding, and arginine mutants of staphylococcal nuclease detected by changes in the enhancement (ϵ^*) of the effects of Mn^{2+} on $1/T_1$ of water protons. (A) Displacement of Mn^{2+} by Ca^{2+} from the binary Mn^{2+} complexes of D40E (◇) and T41P (△). Solutions contained either 262 μM D40E with 118 μM $MnCl_2$ or 193 μM T41P with 125 μM $MnCl_2$. (B) Displacement of Mn^{2+} by Ca^{2+} from the complexes of D21E (□) and D21Y (○). The solutions contained 233 μM D21E with 100 μM $MnCl_2$ or 432 μM D21Y with 118 μM $MnCl_2$. (C) Displacement of Mn^{2+} by Ca^{2+} from the binary complexes of wild-type (●) and arginine mutants R35G (▽) and R87G (×) of staphylococcal nuclease. The solutions contained 179 μM wild-type enzyme with 332 μM $MnCl_2$, 562 μM R35G with 92 μM $MnCl_2$, or 215 μM R87G with 118 μM $MnCl_2$. Other components and conditions are as described in Figure 4. In all cases, Ca^{2+} additions were made from concentrated stock solutions, which also contained all of the other components of the titration solutions at the same final concentrations. K_D^{Ca} was calculated from the concentration of free Ca^{2+} at the midpoint of each titration, $[Ca^{2+}]_{1/2}$, using the relationship $K_D^{Ca} = [Ca^{2+}]_{1/2}/(1 + [Mn^{2+}]/K_D^{Mn})$, where K_D^{Mn} is the dissociation constant of Mn^{2+} from the binary enzyme–Mn^{2+} complex (Serpersu et al., 1986b).

half of the bound Mn^{2+}, together with the measured dissociation constants of the enzyme–Mn^{2+} complexes (Table II), indicate weaker Ca^{2+} binding to all of the liganding mutants by factors ranging from 2.0 for D21E to 12.7 for D40E. The dissociation constants of the binary enzyme–Ca^{2+} complexes measured in the binding studies (Table II) are in reasonable agreement with the activator constants of Ca^{2+}, determined by kinetic studies of the active enzymes (Table I).

Ternary Enzyme–Mn^{2+}–3′,5′-pdTp Complexes of Liganding Mutants. (A) Titrations with Mn^{2+}. To determine K_A', the dissociation constant of Mn^{2+} from ternary enzyme–Mn^{2+}–pdTp complexes, the nuclease mutants were titrated with Mn^{2+} in the presence of 3′,5′-pdTp, a substrate analogue and potent competitive inhibitor (Cuatrecasas et al., 1967b; Dunn & Chaiken, 1975), measuring the free Mn^{2+} concentration by EPR and the enhancement of the effects of bound Mn^{2+} on $1/T_{1P}$ of water protons. To avoid the formation of excessive amounts of binary Mn^{2+}–pdTp complexes, it was necessary to carry out these titrations at equimolar levels of the enzyme and pdTp. While this limitation resulted in subsaturating levels of pdTp at the outset of some titrations, during the course of these titrations the ternary complex was the major species which formed. The validity of this method of estimating K_A' is indicated by the consistency of the K_A' values with values of K_3 and K_S, and of the ϵ_T values measured independently by titrations with pdTp (see below).

Scatchard plots of both the EPR data (Figure 6A) and the $1/T_{1P}$ data (not shown) yielded approximately one tight binding site for Mn^{2+} with the K_A' values listed in Table III. The n and K_A' values obtained by both methods showed good agreement. A comparison of these K_A' values with the respective K_D values (Table II) indicates that the substrate analogue 3′,5′-pdTp significantly raises the affinity of Mn^{2+} for wild-type staphylococcal nuclease and for all of the liganding mutants, by factors ranging from 19 (D21E) to 97 (D40E), consistent with the formation of ternary enzyme–

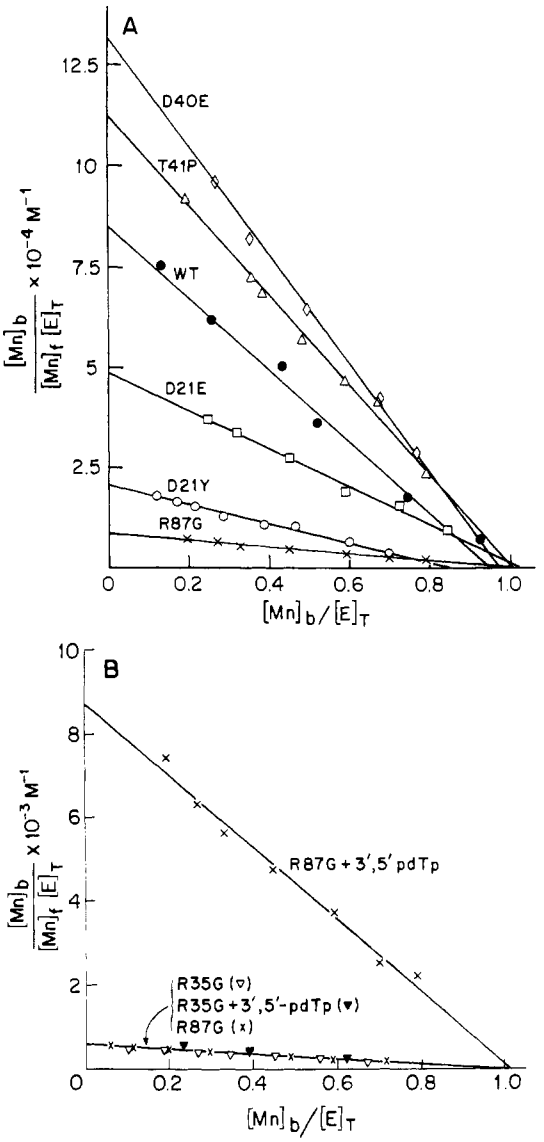

FIGURE 6: Scatchard plots of Mn^{2+} binding to the wild-type, liganding, and arginine mutants of staphylococcal nuclease in the presence of 3',5'-pdTp. (A) Titration of wild-type, liganding mutants and R87G with Mn^{2+}. The solutions contained 85 μM wild type with 85 μM pdTp (●), 20 μM D40E with 20 μM pdTp (◇), 52 μM T41P with 54 μM pdTp (△), 74 μM D21E with 66 μM pdTp (□), 54 μM D21Y with 46 μM pdTp (○), or 179 μM R87G with 176 μM pdTp (×). Other components and conditions are as described in Figure 4. (B) Differential effect of the presence of 3',5'-pdTp on the titrations of R35G and R87G with Mn^{2+}. The data are shown together with the binary Mn^{2+} titration data from Figure 4B for comparison. In (A) and (B), the free Mn^{2+} concentrations were determined by EPR spectroscopy, and the linear least-squares fitted lines are shown together with the data points. The symbols $[Mn]_b$, $[Mn]_f$, and $[E]_T$ represent bound $[Mn^{2+}]$, free $[Mn^{2+}]$, and total enzyme concentrations, respectively.

Mn^{2+}–3',5'-pdTp bridge complexes in each case. The D40E and T41P mutants show slight decreases in K_A' below that of the wild type, while the other liganding mutants show small increases in K_A', the largest change being in K_A' of the D21Y mutant which is 3.2-fold greater than that of the wild type. For those liganding mutants which have catalytic activity, a comparison of the K_A' values determined by binding studies (Table III) with the K_I values of Mn^{2+} determined kinetically (Table I) shows reasonable agreement, considering the structural differences between 3',5'-pdTp and DNA.

(B) Titrations with 3',5'-pdTp. The most direct way of determining K_3, the dissociation constant of 3',5'-pdTp from

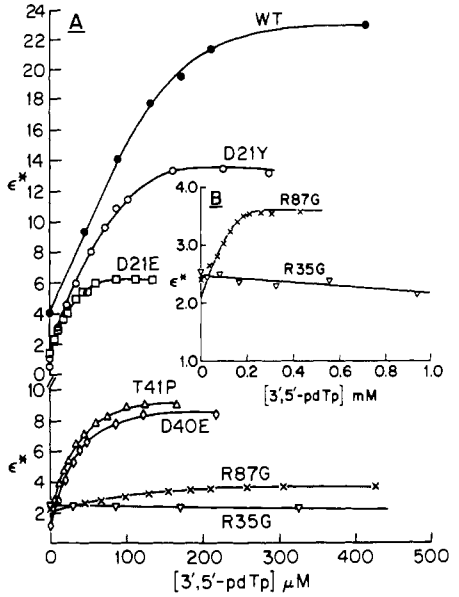

FIGURE 7: Binding of the nucleotide 3',5'-pdTp to the wild-type, liganding, and arginine mutants of staphylococcal nuclease, measuring the changes in the enhancement (ϵ^*) of the paramagnetic effects of Mn^{2+} on $1/T_1$ of water protons. (A) Titration of Mn^{2+} complexes of the wild-type and all of the mutant enzymes with 3',5'-pdTp. The solutions contained 488 μM wild type with 106 μM $MnCl_2$ (●), 162 μM D21Y with 47 μM $MnCl_2$ (○), 56 μM D21E with 25 μM $MnCl_2$ (□), 54 μM T41P with 25 μM $MnCl_2$ (△), 52 μM D40E with 38 μM $MnCl_2$ (◇), 213 μM R87G with 92 μM $MnCl_2$ (×), or 199 μM R35G with 92 μM $MnCl_2$ (▽). Nucleotides were added from concentrated stock solutions, which also contained the other components of the titration at the same final concentrations. Other components and conditions were as described in Figure 5. (B) The data in (A) for the Arg mutants R35G and R87G are replotted in expanded form to show the difference in the effects of 3',5'-pdTp. In both (A) and (B), except for R35G, the data points are shown together with curves computed by using the parameters given in Tables II and III. In the case of R35G, no ternary complex is detected by this method.

the ternary enzyme–Mn^{2+}–nucleotide complex, is by titration of solutions of enzyme and Mn^{2+} with the nucleotide, measuring changes in the enhancement (ϵ^*) of $1/T_{1P}$ of water protons (Serpersu et al., 1986b; Mildvan & Engle, 1972). Such titrations, fit by computed curves (Figure 7A), yielded the average K_3 values for 3',5'-pdTp given in Table III. The computer fitting of these titrations required values for K_S, the dissociation constants of the binary enzyme–3',5'-pdTp complexes (Table III). These are found by trial and error and can therefore be considered only as approximations. Nevertheless, by carrying out such nucleotide titrations at at least two Mn^{2+} concentrations with every mutant, self-consistent values of K_S were obtained. In the case of the wild-type enzyme, the D40G mutant (Serpersu et al., 1986b), and the D21E mutant (Table III), we have shown that K_S values obtained by such titrations agree with those measured directly by fluorescence titrations in competition with 3',5'-ϵpAp.

Comparisons of K_S and K_3 (Table III) indicate that Mn^{2+} raises the affinities of the wild-type enzyme and of all the liganding mutants for 3',5'-pdTp by 1–2 orders of magnitude, again suggestive of the formation of enzyme–Mn^{2+}–nucleotide bridge complexes in each case. Although the effects are smaller, such tightening by Ca^{2+} of DNA binding in the steady state is also seen in the kinetic data since $K_M^{DNA} < K_S^{DNA}$ in all cases (Table I).

Except for the mutations at Asp-21, the liganding mutants show only small changes in K_3 ($\leq$4.5-fold) and K_S ($\leq$1.8-fold) from that of the wild type, as might be expected for changes at residues which do not interact directly with the substrate.

Table III: Dissociation Constants (μM) and Enhancement Factors of $1/T_{1P}$ in Ternary Enzyme–Mn^{2+}–3′,5′-pdTp Complexes of Wild-Type and Mutant Staphylococcal Nucleases[a]

	K_A'		K_S		K_3	K_2	
enzyme	EPR	$1/T_{1P}$[b]	fluorescence[c]	$1/T_{1P}$[d]	$1/T_{1P}$[d]	$1/T_{1P}$[d]	ϵ_T[d]
wild type	11 ± 0.6	17.0 ± 2.0	95 ± 22	94 ± 38	2.5 ± 1.0	2.2 ± 0.9	24.8 ± 0.4
D40G	25.1 ± 2.9	22.6 ± 2.6	60 ± 35	61 ± 30	1.2 ± 0.6	3.2 ± 1.7	8.1 ± 0.6
D40E	7.4 ± 0.3	6.7 ± 1.0		51.1 ± 18	0.56 ± 0.25	0.8 ± 0.37	13.0 ± 1.6
T41P	9.0 ± 0.9	9.6 ± 0.8		67 ± 6.0	2.4 ± 0.4	1.27 ± 0.3	13.3 ± 1.2
D21E	21.0 ± 1.6	20.3 ± 2.8	9.4 ± 3.4	4.6 ± 0.5	0.50 ± 0.18	0.42 ± 0.15	11.1 ± 1.2
D21Y	41.0 ± 3.5	48.6 ± 4.7		17.4 ± 6.0	0.31 ± 0.1	1.5 ± 0.6	19.5 ± 2.3
R35G			900 ± 140[c]		800 ± 200[c]	1600 ± 400[c]	
	766 ± 108[e]	809 ± 129[e]		>1000[e,f]	≥1000[f]	≥2000[f]	
R87G	117 ± 9.0	175 ± 44	63 ± 21	52.5 ± 13	7.2 ± 1.9	13.0 ± 4.0	7.0 ± 0.8

[a] The dissociation constants of the ternary and relevant binary complexes of enzyme (E), metal (M), and ligands (L) are defined as follows (Mildvan & Cohn, 1966): K_1 = [M][L]/[M–L]; K_D = [E][M]/[E–M]; K_2 = [E][M–L]/[E–M–L]; K_A' = [E–L][M]/[E–M–L]; K_3 = [E–M]-[L]/[E–M–L]; K_S = [E][L]/[E–L]. Note that $K_1K_2 = K_3K_D = K_A'K_S$. The parameters for the wild type and D40G are from Serpersu et al. (1986b). [b] Determined by $1/T_{1P}$* of water protons in Mn^{2+} titrations. [c] Determined by titrations, measuring the increase in fluorescence of 3′,5′-ɛpAp when it was displaced by 3′,5′-pdTp (Serpersu et al., 1986) using the measured K_S values of the binary enzyme–pAp complexes (μM): wild type, 70 ± 36; D40G, 60 ± 40; D21E, 53 ± 28; R87G, 154 ± 63; R35G, 147 ± 28. [d] Determined by computer analysis of nucleotide titrations (Figure 7) (Reed et al., 1970; Mildvan & Engle, 1972). [e] K_A' is indistinguishable from K_D^{Mn} (Table II, Figure 6B), indicating no ternary complex formation. [f] Based on the failure to detect ternary complex formation (Figure 7B).

With the D21Y and D21E mutants, 8- and 5-fold decreases, respectively, in K_3 and 5.4- and 13.5-fold decreases, respectively, in K_S below that of the wild-type enzyme are observed (Table III), indicating somewhat stronger binding of the substrate analogue 3′,5′-pdTp to these variants. With the kinetically active D21E mutant, such differences do not show up under steady-state conditions with DNA, since K_S^{DNA} and the K_M^{DNA} both agree with those of the wild-type enzyme (Table I). Possibly, the electrostatic repulsion between Asp-21 and the extra negative charge of 3′,5′-pdTp over that found in the phosphodiester group of DNA is diminished in the D21E and D21Y mutants.

A comparison of K_S^{DNA}, determined by kinetic studies (Table I), with K_S^{pdTp}, determined by binding studies (Table III), indicates that the DNA substrate binds more tightly than does the simple mononucleotide to staphylococcal nuclease and to its mutant forms, except for D21E, probably due to a greater number of interactions between the proteins and DNA (Cuatrecasas et al., 1968).

The dissociation constant of Mn^{2+}–pdTp from the ternary complex (K_2), derived from the relationship $K_2 = K_3K_D/K_1$ (Table III), shows small changes (≤2.8-fold) in the liganding mutants from that of the wild type. The only exception is the D21E mutant which binds Mn^{2+}–3′,5′-pdTp 5.2-fold tighter than does the wild type. This effect results from the unusually tight binding of the nucleotide by the D21E mutant as manifested in both the low K_S and low K_3 values.

With the wild-type enzyme and with all of the liganding mutants, the conversion of the binary enzyme–Mn^{2+} complex to the ternary enzyme–Mn^{2+}–pdTp complex increases the enhancement of the effect of bound Mn^{2+} on $1/T_{1P}$ of water protons, i.e., $\epsilon_T > \epsilon_b$ (Figure 7A, Tables II and III). This 1.8–8.1-fold increase in the enhancement due to bound Mn^{2+} as 3′,5′-pdTp is bound reflects alterations in the hydration sphere of the metal. Differences in ϵ_T for the various mutants reflect structural differences in the coordination sphere of Mn^{2+} in the respective ternary complexes (Table III), analogous to differences found for the binary complexes (Table II). The nature of these changes will be considered in a later section.

Ternary Enzyme–Ca^{2+}–3′,5′-pdTp Complexes of Liganding Mutants. Titrations of ternary enzyme–Mn^{2+}–3′,5′-pdTp complexes with Ca^{2+} were carried out by measuring the decrease in ϵ^*, the observed enhancement of $1/T_{1P}$ of water protons (Figure 8A,B) resulting from the displacement of Mn^{2+} by Ca^{2+}, as independently established by EPR which showed the appearance of free Mn^{2+}. Analysis of these titrations yielded dissociation constants (K_A') of Ca^{2+} from the ternary enzyme–Ca^{2+}–3′,5′-pdTp complexes (Table IV). These values, together with those of K_D, K_1, and K_S (Tables II and III), were used to calculate the remaining dissociation constants K_2 and K_3 to complete the thermodynamic analysis of the six dissociation constants for all of the ternary enzyme–Ca^{2+}–3′,5′-pdTp complexes (Table IV).

Table IV: Dissociation Constants (μM) of Ternary Enzyme–Ca^{2+}–3′,5′-pdTp Complexes of Wild-Type and Mutant Staphylococcal Nucleases[a]

enzyme	K_A'	K_3	K_2
wild type	71 ± 8	13.1 ± 5.8	5.6 ± 1.9
D40G	259 ± 33	9.5 ± 5.1	13.0 ± 7.0
D40E	220 ± 30	1.7 ± 0.7	9.4 ± 3.8
T41P	207 ± 46	4.6 ± 1.1	11.6 ± 3.1
D21E	184 ± 41	1.7 ± 0.7	1.4 ± 0.8
D21Y	1390 ± 200	7.0 ± 3.1	20.2 ± 15.4
R35G	3780 ± 290[b]	1450 ± 400[c]	4760 ± 3000[d]
R87G	1420 ± 380	16.2 ± 5.9	62.1 ± 43

[a] The dissociation constants of the ternary and relevant binary complexes of enzyme, metal, and ligands are defined in Table III. The K_1 value is given in Table II, and the K_S values are given in Table III. The dissociation constants for the wild type and D40G are from Serpersu et al. (1986b). [b] K_A' is indistinguishable from K_D^{Ca} (Table II), indicating weak ternary complex formation. [c] Based on $K_A'K_S/K_D$ (Tables II and III). [d] Based on $K_A'K_S/K_1$ (Tables II and III).

As was found with Mn^{2+}, $K_A'^{Ca} < K_D^{Ca}$ in all cases, indicating that the substrate analogue 3′,5′-pdTp raises the affinity of Ca^{2+} for wild-type staphylococcal nuclease and for all of the liganding mutants by factors ranging from 2.5 (D21Y) to 29.5 (D40E). These data are consistent with the formation of enzyme–Ca^{2+}–3′,5′-pdTp bridge complexes of the wild-type enzyme and of all of the liganding mutants, in accord with the X-ray structure of the ternary complex (Cotton et al., 1979).

Unlike the kinetically determined K_M^{DNA} and K_S^{DNA} which vary by factors of at most 3-fold among the wild-type enzyme and the various liganding mutants, K_3^{pdTp} and K_S^{pdTp} show ≤13.5-fold changes (Table III), reflecting larger differences in affinity for the substrate analogue.

Kinetic Studies of the Arg Mutants of Staphylococcal Nuclease. Mutations at Arg-35 or Arg-87, which are believed to interact with the phosphodiester group of the bound substrate (Cotton et al., 1979), profoundly inhibit enzymatic activity. Thus, the R35G and R87G mutants showed no activity in the standard assay at enzyme levels up to 24 and 28 μg/mL, respectively. Variation of the concentration of Ca^{2+}

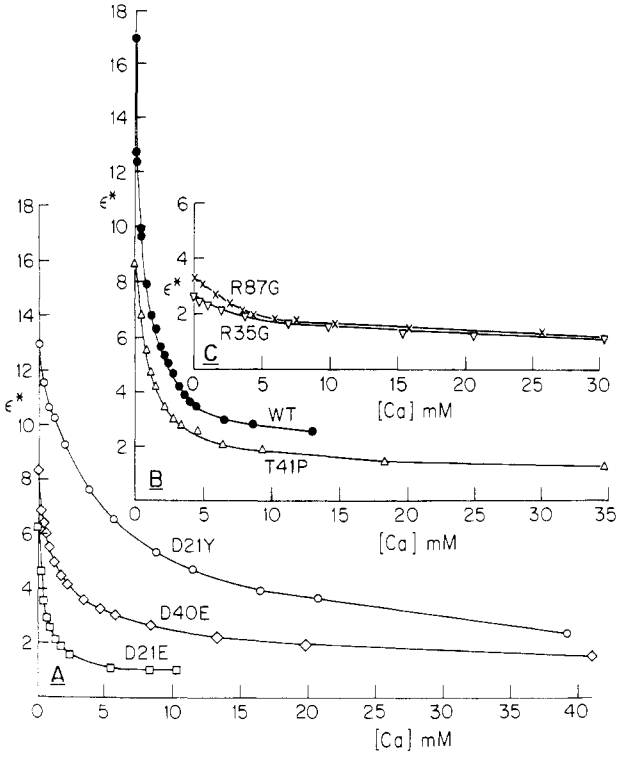

FIGURE 8: Displacement of Mn^{2+} by Ca^{2+} from the ternary enzyme–Mn^{2+}–pdTp complexes of wild-type, liganding, and arginine mutants of staphylococcal nuclease detected by changes in the enhancement (ϵ^*) of the effects of Mn^{2+} on $1/T_1$ of water protons. (A and B) Displacement of Mn^{2+} by Ca^{2+} from the ternary complexes of wild-type enzyme and the liganding mutants. The solutions contained 85 μM wild-type enzyme with 60 μM $MnCl_2$ and 85 μM pdTp (●), 54 μM T41P with 25 μM $MnCl_2$ and 54 μM pdTp (△), 162 μM D21Y with 62 μM $MnCl_2$ and 161 μM pdTp (○), 52 μM D40E with 38 μM $MnCl_2$ and 54 μM pdTp (◇), or 56 μM D21E with 25 μM $MnCl_2$ and 54 μM pdTp (□). (C) Displacement of Mn^{2+} by Ca^{2+} from the complexes of Arg mutants. The solutions contained either 179 μM R87G with 92 μM $MnCl_2$ and 175 μM pdTp or 199 μM R35G with 92 μM $MnCl_2$ and 195 μM pdTp. Other components and conditions were as described in Figure 5. $K_A'^{Ca}$ was calculated from the concentration of free Ca^{2+} at the midpoint of the titration, $[Ca^{2+}]_{1/2}$, using the relationship $K_A'^{Ca} = [Ca^{2+}]_{1/2}/(1 + [Mn^{2+}]/K_A'^{Mn})$, where $K_A'^{Mn}$ represents the dissociation constant of Mn^{2+} from the ternary enzyme–metal–nucleotide complex (Table III) (Serpersu et al., 1986b). In the case of R35G, $K_A'^{Mn} = K_D^{Mn}$, indicating no detectable ternary complex formation with this mutant as also found by the titration in Figure 7.

from 0.2 μM to 50 mM, and of DNA concentration from 29 to 97.5 μg/mL, produced no detectable activity, indicating the k_{cat} of the R35G and R87G mutants to be at least 35 700-fold lower than that of the wild-type enzyme at pH 7.4 (Table I). Accordingly, the semiquantitative plate assay revealed very low levels of activity, with R35G 50 000-fold less active and R87G 31 000-fold less active than the wild-type enzyme at pH 9.0.[2]

Binary Mn^{2+} and Ca^{2+} Complexes of the Arg Mutants of Staphylococcal Nuclease. Binding studies of Mn^{2+} to the R35G and R87G mutants, as measured by EPR (Figure 4B) and by $1/T_{1P}$ of water protons, yield dissociation constants (K_D^{Mn}) only 2-fold greater and enhancement factors (ϵ_b) very similar to those of the wild-type enzyme (Table II). These findings indicate very small changes in the hydration sphere of Mn^{2+} in the binary complexes of the Arg mutants. With the larger Ca^{2+} ion, binding studies in competition with Mn^{2+} (Figure 5C) yield K_D^{Ca} values for R35G and R87G which are, respectively, 7.7- and 9.0-fold greater than that of the wild-type enzyme (Table II), suggesting structural changes in the Arg mutants.

Although no X-ray structure of the binary enzyme–Ca^{2+} complex exists, the 2.0-Å structue of the free enzyme shows the metal ligands Asp-40 and Asp-21 to be buried, with Asp-21 hydrogen bonded to Arg-35 and Arg-87 exposed to solvent (Tucker et al., 1979; Stanislowski, 1976). A comparison of this structure with that of the ternary enzyme–Ca^{2+}–3′,5′-pdTp complex (Tucker et al., 1979; Stanislowski, 1976) reveals that the binding of the Ca^{2+}–nucleotide complex to the enzyme breaks the hydrogen bond between Arg-35 and Asp-21, allowing Arg-35 to move 2 Å toward the 5′-phosphate of pdTp and Asp-21 to coordinate the metal. Asp-40, in coordinating the Ca^{2+}, becomes more exposed to solvent while Arg-87 becomes less so, as it approaches the nucleotide. A computer graphics study of the ternary complex shows Arg-35 to be in the second coordination sphere of the metal with a guanidinium nitrogen 4.5 Å from Ca^{2+} and Arg-87 to be in the third coordination sphere of the metal with a guanidinium nitrogen 7.7 Å from Ca^{2+}. From these observations, the loss of a positive charge near Ca^{2+} in the R35G and R87G mutants would be expected to decrease K_D^{Mn} and K_D^{Ca}, if no other structural changes had occurred. The small increases in K_D which are observed (Table II) indicate that the electrostatic effects of the removal of Arg are exceeded by the effects of the structural alterations in the Arg mutants. However, since ϵ_b shows only very small changes in these mutants, it is reasonable to suggest that these structural changes are primarily in the apoenzymes rather than in the binary metal–enzyme complexes.

Ternary Mn^{2+} and Ca^{2+} Complexes of the Arg Mutants of Staphylococcal Nuclease with 3′,5′-pdTp. Titration of R87G mutant with Mn^{2+} in the presence of 3′,5′-pdTp (Figure 6B) yields a K_A' value (Table III) which is (6 ± 1)-fold lower than K_D^{Mn} (Table II), indicating that 3′,5′-pdTp raises the affinity of the R87G mutant for Mn^{2+}. These data are consistent with the formation of a ternary enzyme–Mn^{2+}–3′,5′-pdTp complex, as found with the wild-type enzyme and with all of the liganding mutants. Independent evidence for ternary complex formation is provided by titration of the binary Mn^{2+} complex of R87G with 3′,5′-pdTp, measuring the increasing enhancement factor (ϵ^*) of $1/T_{1P}$ of water protons (Figure 7B). The computed titration curve (Figure 7B) yields a dissociation constant (K_3) of 3′,5′-pdTp from the ternary complex of the R87G mutant only 2.9-fold greater than that of the wild-type enzyme and a dissociation constant (K_S) of the binary enzyme–3′,5′-pdTp complex which is 1.6-fold tighter than that of the wild-type enzyme (Table III). This K_S value was independently measured and confirmed by a fluorescence titration in competition with 3′,5′-ϵpAp (Table III). The ratio of the K_3 and K_S values of the R87G mutant indicates an 8-fold tightening by Mn^{2+} of nucleotide binding to the enzyme. This finding, together with the observation that the ternary enhancement factor (ϵ_T) exceeds that of the binary complex (ϵ_b) (Figure 7B, Tables II and III), establishes the formation of a stable ternary complex of the R87G mutant.

In sharp constrast to the findings with R87G, titration of the R35G mutant with Mn^{2+} in the presence of 3′,5′-pdTp (Fig. 6B) shows no significant change in the affinity of the enzyme for Mn^{2+} induced by the presence of the nucleotide, i.e., $K_A'^{Mn} = K_D^{Mn}$ (Table III). The agreement of K_A' with K_D suggests that 3′,5′-pdTp does not bind detectably to the Mn^{2+} complex of the R35G mutant to form a strong ternary complex. This point was reinforced by a titration of the binary Mn^{2+} complex of R35G with 3′,5′-pdTp (Figure 7B) which showed no significant increase in the enhancement (ϵ^*) of $1/T_{1P}$ of water protons at nucleotide levels up to 1 mM. The

Table V: Frequency Dependence of Longitudinal Relaxation Rates of Water Protons in the Presence of Mn^{2+} Complexes of Wild-Type and Active-Site Mutants of Staphylococcal Nuclease[a]

complex	$1/fT_{1P}$ ($\times 10^{-6}$ s^{-1}) at frequency (MHz)								$1/fT_{2P}$ ($\times 10^{-6}$ s^{-1}) at frequency (MHz) 24.3
	15	19.7	24.3	30	36	42	50	59.8	
wild type–Mn	2.10	2.17	2.41	2.24	2.05	1.82	1.67	1.45	15.1
wild type–Mn–pdTp	6.18	6.31	6.57	6.03	5.54	4.91	4.21	3.47	7.76
D40G–Mn	2.66	2.80	2.87	2.68	2.63	2.65	2.49	2.39	18.1
D40G–Mn–pdTp	4.19	4.47	5.00	4.26	3.97	3.72	3.28	2.85	5.12
D40E–Mn	0.996	1.15	1.31	1.21	1.18	1.09	0.947	0.902	4.49
D40E–Mn–pdTp	4.43	4.56	4.34	4.41	4.13	3.81	3.36	2.86	4.73
T41P–Mn	1.77	1.85	1.98	1.97	1.80	1.64	1.54	1.40	4.16
T41P–Mn–pdTp	4.38	4.56	4.35	4.35	4.05	3.52	3.05	2.57	5.60
D21E–Mn	1.01	1.16	1.24	1.15	1.14	1.02	0.901	0.761	3.79
D21E–Mn–pdTp	2.22	2.42	2.49	2.52	2.48	2.34	2.11	1.87	3.07
D21Y–Mn	1.25	1.30	1.21	1.10	1.08	1.01	1.02	1.03	15.1
D21Y–Mn–pdTp	5.07	4.89	4.99	4.56	4.65	4.63	4.57	3.92	8.35
R35G–Mn	3.42	3.67	4.05	3.87	3.62	3.47	3.21	2.85	10.6
R87G–Mn	2.45	2.59	2.82	2.65	2.53	2.36	2.22	1.93	10.2
R87G–Mn–pdTp	2.18	2.24	2.15	2.20	2.09	1.92	1.81	1.52	7.18

[a] For all the frequencies, the normalized longitudinal relaxation rates of water protons ($1/fT_{1P}$) and for 24.3-MHz normalized transverse ($1/fT_{2P}$) relaxation rates are given, where $f = [Mn]_b/[H_2O]$.

small decrease observed in ϵ^* can be explained by the removal of Mn^{2+} from the enzyme by 3′,5′-pdTp to form a mixture of binary complexes of the nucleotide and the enzyme. From the titration data of Figure 7B, it is estimated that if a ternary complex of the R35G mutant had formed, its dissociation constant K_3 must be ≥ 1 mM. If a binary enzyme–3′,5′-pdTp complex had formed, its dissociation constant K_S must also be ≥ 1 mM since $K_S = K_3K_D/K_A'$ and $K_D \sim K_A'$ for the R35G mutant (Figure 6B, Table III). From these limits and from the measured values of K_D and K_1, a lower limit to $K_2 \geq 2$ mM is obtained. Consistent with these limiting values, only very weak binding of 3′,5′-pdTp to R35G and to its Mn^{2+} complex was detected by the fluorescence titrations (Table III). It is concluded that while both of the Arg mutants R35G and R87G bind Mn^{2+} tightly, only the R87G mutant binds the substrate analogue 3′,5′-pdTp with normal affinity. The Mn^{2+} complex of the R35G mutant binds 3′,5′-pdTp 320-fold more weakly than does the wild-type enzyme.[4]

Very similar results were obtained in studies of the ternary Ca^{2+} complexes of the Arg mutants. With the R87G mutant, Mn^{2+} displacement titrations by Ca^{2+} in the presence of 3′,5′-pdTp (Figure 8C) yield a K_A' for Ca^{2+} (Table IV) which is 3.2-fold lower than K_D^{Ca} (Table II). This increase in affinity for Ca^{2+} by 3′,5′-pdTp indicates the formation of a ternary enzyme–Ca^{2+}–nucleotide complex. The dissociation constant of 3′,5′-pdTp from this ternary complex (K_3) is indistinguishable from that of the wild-type enzyme (Table IV). However, with the R35G mutant, Mn^{2+} displacement titrations with Ca^{2+} in the presence of 3′,5′-pdTp (Figure 8C) yield a K_A' (Table IV) which is equal to K_D^{Ca} (Table II), indicating no detectable formation of a ternary complex. If very weak binding of 3′,5′-pdTp to the R35G mutant or to its Ca^{2+} complex had occurred, lower limit values to the dissociation constants of the nucleotide (K_S and K_3) are estimated to be in the millimolar range. Accordingly, fluorescence titrations yield a K_3 value which is more than 100-fold weaker than that found with the wild-type enzyme (Table IV).[4]

Frequency Dependence of $1/T_{1P}$ of Water Protons with Binary and Ternary Mn^{2+} Complexes of Staphylococcal Nuclease Mutants. As previously shown for the wild-type enzyme and for the D40G mutant (Serpersu et al., 1986b), the enhancement factor increases on conversion of the binary enzyme–Mn^{2+} complex to the ternary enzyme–Mn^{2+}–pdTp complex ($\epsilon_T > \epsilon_b$), and this effect results from an increase in both the correlation time τ_c and the number of fast-exchanging water ligands. The present data (Figure 7, Tables II and III) indicate that $\epsilon_T > \epsilon_b$ for all of the mutants in which a ternary complex has formed. With the exception of the R35G mutant, the enhancement factors of the binary Mn^{2+} complexes (ϵ_b) of all of the mutants studied are lower than that of the wild-type enzyme (Table II), and in all cases in which a ternary enzyme–Mn^{2+}–3′,5′-pdTp complex has formed, the ternary enhancement factors (ϵ_T) of the mutants are lower than that of the wild-type enzyme (Table III).

To determine the mechanism of these effects, the frequency dependence of the paramagnetic effects of enzyme-bound Mn^{2+} on $1/T_1$ of water protons was measured (Table V). In these studies, eight frequencies over the most sensitive range were used. For comparison, the measurements on the wild-type enzyme and the D40G mutant were repeated, with similar results (Table V; Serpersu et al., 1986b). The observation that $1/fT_{2P}$ significantly exceeds $1/fT_{1P}$ in most cases, and that $1/fT_{1P}$ is frequency dependent (Table V), indicates that $1/fT_{1P}$ does not include a major contribution from $1/\tau_M$, the chemical exchange rate of water ligands. As indicated by the low errors in Table VI ($\leq 5.5\%$), good fits to the $1/fT_{1P}$ data have been obtained without adding τ_M as an additional parameter. As seen in Table V, in nearly all complexes $1/fT_{1P}$ reaches a maximum between 19.7 and 30 MHz, indicating that τ_c is dominated by the electron-spin relaxation time of Mn^{2+} (Reuben & Cohn, 1970; Bloembergen & Morgan, 1961).

Analysis of these data (Table VI) indicates that the increase in the relaxivity of the bound Mn^{2+} upon conversion of binary to ternary complexes is accompanied by an increase in τ_c in all but the D21E mutant, and by an increase in q in all but the D21Y and R87G mutants. The increases in τ_c, when present, result from a decrease in B, the zero-field splitting parameter, indicating an increase in the symmetry of the ligand field at Mn^{2+} on formation of the ternary complexes. The increases in q on formation of the ternary complexes indicate a more facile exchange of water ligands of Mn^{2+} with the bulk solvent. The values of q, which represent the number of fast-exchanging water ligands on bound Mn^{2+}, are significantly lower than predicted from the X-ray structure (Figure 1)

[4] The fact that R35G shows detectable activity in the plate assay (50 000-fold below that of the wild type) indicates that DNA can bind to the Ca^{2+} complex of R35G.

Table VI: Analysis of Frequency Dependence of Longitudinal Relaxation Rates of Water Protons in the Presence of Mn^{2+} Complexes of Staphylococcal Nuclease and Its Mutants[a]

complex	τ_c ($\times 10^9$ s)	B ($\times 10^{-20}$ s^{-2})	τ_v ($\times 10^{13}$ s)	q	error (%)
wild type–Mn	2.25	1.42	6.34	0.78	4.7
wild type–Mn–pdTp	2.87	0.89	7.94	1.77	3.0
D40G–Mn	1.29	1.79	8.89	1.50	3.5
D40G–Mn–pdTp	2.26	1.26	7.11	1.61	5.5
D40E–Mn	1.60	2.01	6.29	0.56	6.3
D40E–Mn–pdTp	2.52	1.78	4.47	1.42	3.1
T41P–Mn	1.83	1.13	10.0	0.76	4.0
T41P–Mn–pdTp	2.59	0.79	8.9	1.26	3.3
D21E–Mn	1.93	0.56	21.2	0.45	5.5
D21E–Mn–pdTp	1.80	0.63	19.9	0.97	2.7
D21Y–Mn	0.287	15.6	4.5	2.73	4.1
D21Y–Mn–pdTp	1.60	0.71	20.0	2.15	3.3
R35G–Mn	2.03	1.26	7.94	1.42	4.0
R87G–Mn	2.07	0.89	11.2	0.97	3.8
R87G–Mn–pdTp	2.16	0.63	15.8	0.71	2.8

[a] The normalized longitudinal relaxation rates of water protons ($1/fT_{1P}$) as a function of the precession frequencies of protons (ω_I) and unpaired electrons (ω_S) were analyzed according to the following equations (Mildvan & Gupta, 1978): $1/fT_{1P} = q(C/r)^6[3\tau_c/(1 + \omega_I^2\tau_c^2) + 7\tau_c/(1 + \omega_S^2\tau_c^2)]$ and $1/\tau_c \sim 1/\tau_S = B[\tau_v/(1 + \omega_S^2\tau_v^2) + 4\tau_v/(1 + 4\omega_S^2\tau_v^2)]$, where q is the number of fast-exchanging water ligands, C is a product of physical constants equal to 812 $Å/s^{1/3}$ for Mn^{2+}–proton interactions, τ_c is the dipolar correlation time, τ_S is the longitudinal electron-spin relaxation time, B is the zero field splitting parameter, and τ_v is a time constant for motion of the water ligands which modulates B (Friedman, 1977). The data were collected at the frequencies shown in Table VI, and the dipolar correlation time (τ_c) is given for 24.3 MHz.

except for the binary and ternary complexes of D21Y and the ternary complexes of the wild-type and the D40G mutant (Table V). These findings suggest that one or two water ligands of Mn^{2+} exchange very slowly ($<10^6$ s^{-1}) with the bulk solvent in most cases.

The decreased relaxivity of Mn^{2+} when bound in binary and ternary complexes of the mutant enzymes as compared to the wild-type enzyme is due, in all cases, to lower correlation times with the mutants. The lower τ_c values or electron-spin relaxation times result from a change in the symmetry (B) and/or the time constant for motion (τ_v) of the ligands of Mn^{2+} (Table V), reflecting detailed structural alterations in the coordination sphere of the metal.

Discussion

With the exception of the R87G mutant, the kinetic, thermodynamic, and structural effects of mutations of the active-site residues are in accord with the X-ray structure of the nuclease–Ca^{2+}–3′,5′-pdTp complex and with the mechanism based on this structure (Figure 2). Thus, alterations of the metal ligands generally result in, at most, an order of magnitude weakening of the affinity of the enzyme for Mn^{2+} or Ca^{2+} (Table II), an order of magnitude change in affinity for the substrate analogue 3′,5′-pdTp (Tables III and IV), and, when measurable, small increases (≤3-fold) in the K_S^{DNA} and K_M^{DNA} (Table I). Similarly, relatively small changes in the affinity of the enzyme for Mn^{2+} (2-fold) or Ca^{2+} (≤9-fold) result from deletion of the catalytically essential Arg residues in the R35G and R87G mutants (Table II). In contrast to these small effects on dissociation constants, much greater effects of the amino acid changes on k_{cat} are observed, altering it by at least 3–5 orders of magnitude relative to that of the wild-type enzyme (Table I).

The one mutant which displays a large change in substrate binding is R35G. This enzyme shows very little activity[2] and very weak binding of the substrate analogue 3′,5′-pdTp, either

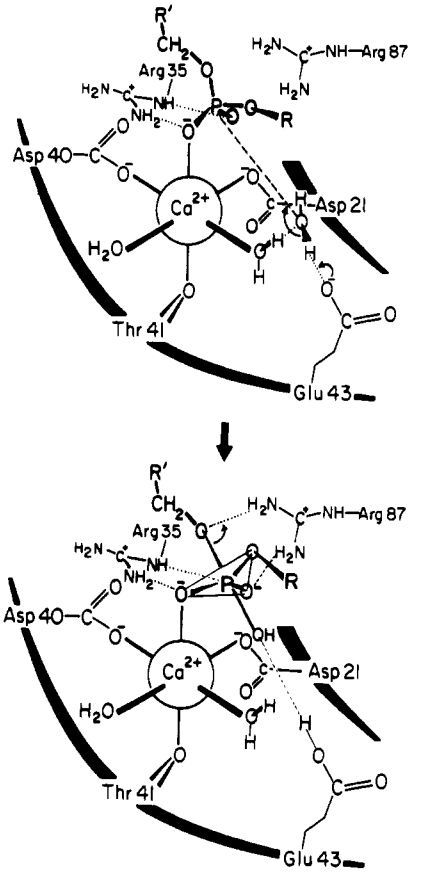

FIGURE 9: Modified reaction mechanism of staphylococcal nuclease based on studies with liganding and arginine mutants. In the initial complex (upper), the tetrahedral phosphodiester of the substrate interacts with Ca^{2+} and with Arg-35 but not with Arg-87. When the trigonal bipyramidal transition state forms (lower), Arg-87 then interacts, donating hydrogen bonds and neutralizing the additional negative charge of the phosphorane to stabilize the transition state.

to free enzyme or to its metal complexes, indicating dissociation constants for this ligand which are at least 2 orders of magnitude greater than those of wild type (Tables III and IV).[4] These large kinetic and thermodynamic effects are consistent with the suggested role of Arg-35 as the donor of a strong bifunctional hydrogen bond to the tetrahedral phosphodiester group of the substrate (Figure 2).

However, the corresponding substitution of Arg-87 in the R87G mutant, which also profoundly reduces activity, results in no significant change in the affinity of the substrate analogue 3′,5′-pdTp for the enzyme or for its metal complexes, from that found with the wild-type enzyme. This finding is contrary to the conclusions of the X-ray analysis (Cotton et al., 1979) and to the mechanism of Figure 2, in which Arg-87 also donates a strong, bifunctional hydrogen bond to the tetrahedral phosphodiester group of the substrate. Nevertheless, Arg-87 is clearly essential for catalysis since the R87G mutant is reduced in k_{cat} by a factor of $\geq 10^{4.6}$ (Table I). It may therefore be reasonably suggested that Arg-87 interacts with the trigonal bipyramidal transition state rather than with the tetrahedral ground state of the bound DNA substrate, as depicted in the modified mechanism of Figure 9. The kinetic data suggest that such transition-state stabilization by Arg-87 contributes a factor of $\geq 10^{4.6}$ to catalysis.

The mechanism of Figure 9 is preferable to that of Figure 2 for another reason, since it preserves electroneutrality at the reaction center phosphodiester throughout the course of the reaction. Thus, the divalent cation Ca^{2+} is neutralized by Asp-21 and Asp-40. The phosphodiester, which is a mo-

noanion in the ground state, is neutralized by the guanidinium cation of Arg-35 only. As the entering hydroxide bonds to phosphorus, converting the reaction center from a phosphodiester monoanion to a phosphorane dianion, a second guanidinium cation, that of Arg-87, is needed to neutralize the additional negative charge which develops in the transition state (Figure 9). Such development of additional negative charge on the equatorial oxygens of the transferred nucleotidyl group in the transition state is characteristic of an associative nucleophilic substitution at phosphorus. The other major criteria of an associative mechanism, general base catalysis and a reaction coordinate distance <4.9 Å (Mildvan & Fry, 1987), are also met by the mechanism of Figure 9.

The mechanism of Figure 9 permits us to utilize the kinetic effects of the active-site mutants of staphylococcal nuclease (Table I) to quantitatively separate the factors contributing to the $\sim 10^{16}$-fold rate acceleration of phosphodiester hydrolysis (k_{cat}) produced by this enzyme. We choose to discuss k_{cat} rather than k_{cat}/K_M since the latter contains binding parameters, and little is known about the detailed binding interactions of DNA or even of oligonucleotides with staphylococcal nuclease. To utilize the effects on k_{cat} of genetic modification of specific residues to quantitatively explain an overall rate enhancement, two conditions must be met. (1) The catalytic and structural effects of each mutation must be limited to the residue altered. (2) Each specific contribution to the rate enhancement must be independent and counted only once. While thermodynamic evidence is here presented for structural alterations beyond the residues changed by mutation, these indirect effects on dissociation constants are small, generally within an order of magnitude of the wild-type enzyme, while the kinetic effects on k_{cat} are much greater, often differing by 3–5 orders of magnitude from that of the wild-type enzyme. Because the effects of the mutations studied on the dissociation constants for metals and for the substrate analogue 3′,5′-pdTp are small, significant changes in the active-site region of the ternary complexes are unlikely. On the contrary, the binding data suggest that the overall geometry of the active site has been remarkably well retained in spite of major amino acid residue changes.

Establishing that each contribution to the catalytic rate is independent and counted only once is more difficult. To avoid counting an effect twice, we have made comparisons between complexes with active and inactive metal ions, and between appropriate pairs of mutants, such as D40E with D21E and R35G with R87G. We have begun to address this issue further by NMR studies of the structures of ternary complexes,[3] by analyzing the effects of additional amino acid substitutions at each essential position,[5] and by examining the additivity of effects of pairs of single, well-characterized mutations (Carter et al., 1984; Ackers & Smith, 1985). With the above reservations in mind, we suggest the following quantitative analysis of the 10^{16}-fold rate enhancement produced by staphylococcal nuclease on the basis of the effects on k_{cat} produced by the active-site mutants analyzed in this paper.

As discussed above, transition-state stabilization by Arg-87 (Figure 9) may be assumed to contribute a factor $\geq 10^{4.6}$ to catalysis, since k_{cat} decreases by this factor in the R87G mutant (Table I).

The divalent cation Mn^{2+} occupies the Ca^{2+} binding site of staphylococcal nuclease, on the basis of (1) the competition between Ca^{2+} and Mn^{2+} both in kinetics and in binding studies, (2) the tightening of binding of both metals to the enzyme by DNA, by 3′,5′-pdTp, and (3) the similar effects of mutations of the active-site residues of the enzyme on the affinities for both metals. Despite its location at the Ca^{2+} binding site, Mn^{2+} fails to activate the wild-type enzyme or any of the mutants studied, presumably because of the significantly smaller size of this cation as compared to Ca^{2+}.[3] From the limits of the standard assay, it is estimated that Mn^{2+} is at least $10^{4.6}$-fold less effective than Ca^{2+} in activating the wild-type enzyme. Hence, the proper metal, Ca^{2+} in this case, contributes a factor of at least $10^{4.6}$ to catalysis by staphylococcal nuclease, presumably due to effects on both the ground state and the transition state of the bound phosphodiester substrate (Figure 9). The factor of $\geq 10^{4.6}$ due to Ca^{2+} catalysis may be subdivided into a geometric contribution of $\sim 10^{1.5}$, as suggested by the k_{cat} values of the liganding mutants D40G, D40E, and T41P (Table I), and other effects which contribute $\geq 10^{3.1}$, such as electron withdrawal and substrate immobilization.

A comparison of the k_{cat} values of the D40E mutant, which is 12-fold less active than the wild-type enzyme, with the D21E mutant, which is 1500-fold less active (Table I), reveals a 120-fold greater decrease resulting from the enlargement of Asp-21 than from the identical enlargement of Asp-40. Further enlargement of Asp-21 to tyrosine in the D21Y mutant reduces enzymatic activity by a factor of at least $10^{4.5}$ below that of the wild-type enzyme. The profound sensitivity of k_{cat} to increases in the size of the residue at position 21 presumably results from the fact that this ligand is adjacent to the attacking water molecule (Figures 2 and 9). Model-building studies indicate that, depending on the orientation of its side chain, Glu-21 can partially overlap and Tyr-21 can totally overlap with either the adjacent inner-sphere or the second-sphere water ligand of Ca^{2+}. The appropriate values of q, the number of fast-exchanging inner-sphere water ligands on Mn^{2+} in the binary and ternary enzyme–Mn^{2+}–3′,5′-pdTp complexes of the D21Y mutant (Table VI), suggest that Tyr-21 is not directly coordinated to Mn^{2+}, possibly because it is uncharged, but is probably in the second coordination sphere of the metal, displacing the attacking water ligand.[6] If so, then catalysis by approximation, i.e., by the proper positioning of the attacking water molecule, contributes a factor of $\geq 10^3$, when the $\geq 10^{4.5}$-fold effect of the D21Y mutation is corrected by the geometric effect of enlarging the metal ligand ($10^{1.5}$), based on the k_{cat} values of the D40E and T41P mutants (Table I).

As noted above, Hibler and Gerlt (1986) have observed a $\sim 10^4$-fold decrease in the activity of the E43N mutant, suggesting that general base catalysis by Glu-43 contributes a factor of $\sim 10^4$ to k_{cat} (Figure 9).

Hence, if the indirect effects of the mutations on catalysis are indeed small, and if no catalytic effect has been counted twice, then the product of the contributions of transition-state stabilization by Arg-87 ($\geq 10^{4.6}$), metal catalysis by Ca^{2+} ($\geq 10^{4.6}$), catalysis by approximation ($\geq 10^3$), and general base catalysis ($\sim 10^4$) are sufficient to explain the overall rate acceleration of $\sim 10^{16}$-fold produced by staphylococcal nuclease. The mechanism of Figure 9 may therefore provide a quantitative as well as a qualitative description of catalysis by this enzyme.

ACKNOWLEDGMENTS

We are grateful to Tian Y. Tsong for permitting us to use

[5] The R87C mutant has a k_{cat} which is ≥32 000-fold lower than that of the wild-type enzyme.

[6] Attempts to detect Ca^{2+}-dependent nucleotidyl transfer from DNA to Tyr-21 in the D21Y mutant, by comigration of ^{32}P-labeled DNA with the enzyme in SDS–PAGE, have not been successful.

his spectrofluorometer and to Eric Suchanek for assistance with the computer graphics.

REFERENCES

Ackers, G. K., & Smith, F. R. (1985) *Annu. Rev. Biochem. 54*, 597–629.

Anfinsen, C. B., Cuatrecasas, P., & Taniuchi, H. (1971) *Enzymes (3rd Ed.) 4*, 177–204.

Bloembergen, N., & Morgan, L. O. (1961) *J. Chem. Phys. 34*, 842–850.

Bradford, M. M. (1976) *Anal. Biochem. 72*, 248–254.

Bunton, C. A., Mhala, M. M., Oldham, K. G., & Vernon, C. A. (1960) *J. Chem. Soc. 1960*, 3293–3301.

Carr, H. Y., & Purcell, E. M. (1954) *Phys. Rev. 94*, 630–638.

Carter, P. J., Winter, G., Wilkinson, A. J., & Fersht, A. R. (1984) *Cell (Cambridge, Mass.) 38*, 835–840.

Chaiken, I. M., & Sanchez, G. R. (1972) *J. Biol. Chem. 247*, 6743–6747.

Cleland, W. W. (1979) *Methods Enzymol. 63*, 103–138.

Cohn, M., & Townsend, J. (1954) *Nature (London) 173*, 1090–1091.

Cotton, F. A., Day, V. W., Hazen, E. E., Jr., Larsen, S., & Wang, S. T. K. (1974) *J. Am. Chem. Soc. 96*, 4471–4478.

Cotton, F. A., Hazen, E. E., Jr., & Legg, M. J. (1979) *Proc. Natl. Acad. Sci. U.S.A. 76*, 2551–2555.

Cuatrecasas, P., Fuchs, S., & Anfinsen, C. B. (1967a) *J. Biol. Chem. 242*, 1541–1547.

Cuatrecasas, P., Fuchs, S., & Anfinsen, C. B. (1967b) *J. Biol. Chem. 242*, 3063–3067.

Cuatrecasas, P., Wilchek, M., & Anfinsen, C. B. (1968) *Science (Washington, D.C.) 62*, 1491–1493.

Dunn, B. M., & Chaiken, I. M. (1975) *Biochemistry 14*, 2343–2349.

Dunn, B. M., DiBello, C., & Anfinsen, C. B. (1973) *J. Biol. Chem. 248*, 4769–4774.

Friedman, H. L. (1977) in *Protons and Ions Involved in Fast Dynamic Phenomena* (Laszlo, P., Ed.) p 27, Elsevier, New York.

Hibler, D. W., & Gerlt, J. A. (1986) *Fed. Proc., Fed. Am. Soc. Exp. Biol. 45*, 1875.

Kumamoto, J., Cox, J. R., & Westheimer, F. H. (1956) *J. Am. Chem. Soc. 77*, 4858–4860.

Lachica, R. V. F., Genigeorgis, C., & Hoeprich, P. O. (1971) *Appl. Microbiol. 21*, 585–587.

Mildvan, A. S., & Cohn, M. (1963) *Biochemistry 2*, 910–919.

Mildvan, A. S., & Cohn, M. (1966) *J. Biol. Chem. 241*, 1178–1193.

Mildvan, A. S., & Engle, J. L. (1972) *Methods Enzymol. 26C*, 654–682.

Mildvan, A. S., & Gupta, R. K. (1978) *Methods Enzymol. 49G*, 322–359.

Mildvan, A. S., & Fry, D. C. (1987) *Adv. Enzymol. Relat. Areas Mol. Biol. 59*, 241–313.

Reed, G. H., Cohn, M., & O'Sullivan, W. J. (1970) *J. Biol. Chem. 245*, 6547–6552.

Reuben, J., & Cohn, M. (1970) *J. Biol. Chem. 245*, 6539–6546.

Serpersu, E. H., Shortle, D., & Mildvan, A. S. (1986a) *Fed. Proc., Fed. Am. Soc. Exp. Biol. 45*, 1632.

Serpersu, E. H., Shortle, D., & Mildvan, A. S. (1986b) *Biochemistry 25*, 68–77.

Shortle, D. (1983) *Gene 22*, 181–189.

Shortle, D., & Lin, B. (1985) *Genetics 110*, 539–555.

Slater, J. P., Tamir, I., Loeb, L. A., & Mildvan, A. S. (1972) *J. Biol. Chem. 247*, 6784–6794.

Stanislowski, A. G. (1976) Ph.D. Dissertation, Texas A&M University.

Sulkowski, E., & Laskowski, M., Sr. (1968) *J. Biol. Chem. 243*, 4917–4921.

Tucker, P. W., Hazen, E. E., Jr., & Cotton, F. A. (1978) *Mol. Cell. Biochem. 22*, 67–77.

Tucker, P. W., Hazen, E. E., Jr., & Cotton, F. A. (1979) *Mol. Cell. Biochem. 23*, 67–86.